



Original Article

Influence of welding current in resistance spot welding on the properties of Zn coated steel DX51D

Luboš Kaščák^{1*}, Ján Viňáš¹, and Rudolf Mišičko²

¹ *Department of Technology and Materials, Faculty of Mechanical Engineering*

² *Department of Materials Science, Faculty of Metallurgy,
Technical University of Košice, Košice, Slovakia.*

Received: 4 August 2015; Accepted: 29 October 2015

Abstract

The paper deals with the resistance spot welding of three galvanized car body sheets DX51D + Z - EN 10142/2000. The quality of welded joints was evaluated by destructive tests and non-destructive tests. For evaluation of joints quality the shear tension test on spot joints according to DIN 50 124 standard was used. The influence of welding parameters on the structure of a welded joint was observed by metallographic analysis. Influence of welding current from 6.0 to 7.7 kA and influence of welding time from 10 to 12 periods on weld properties was observed. Increasing the welding current led to increased load-bearing capacity of the welded joints. The spot welded joints without any internal defects occurred in samples welded up to 7.0 kA. Increasing the welding time to 12 periods led to increased load-bearing capacity of the welded joints, within all observed values of welding current.

Keywords: spot welding, quality evaluation, tensile test, metallographic analysis

1. Introduction

Car producers make an effort to achieve the lowest possible fuel consumption, and high active and passive safety of passengers while decreasing the amount of emission.

One of the possibilities of decreasing the car weight and consequently lowering the fuel consumption is using various combinations of materials, such as combination of conventional deep-drawn steel sheet and high-strength steel sheet. In the areas where high passive safety is needed, high-strength steels such as TRIP and DP steels can be used. The usage of such steels can significantly reduce the car weight. Their strength properties allow a reduction the thicknesses of particular segments of a car body (Kaščák, 2007; Hilditch, 2007).

The car body consists of several materials (Figure 1) which need to be joined together to form one unit, usually by welding. Combining various types of materials having different mechanical properties and chemical composition, makes it necessary to consider various methods of welding and joining. Specific demands on the weldability of particular types of materials must be taken into consideration to optimize welding parameters with the aim of eliminating defects in welded joints (Harling, 2003; Zhang, 2006).

Two types of coatings are generally applied to steel sheets used in the automotive industry, namely galvanized and galvaneal coatings. Galvanized coatings contain essentially pure zinc with about 0.3 to 0.6 wt-% aluminium. The term “galvanize” comes from the galvanic protection that zinc provides to steel substrate when exposed to a corroding medium. A galvaneal coating is obtained by additional heating of the zinc-coated steel at 450-590°C (840-1100°F) immediately after the steel exits the molten zinc bath. This additional heating allows iron from the substrate to diffuse

* Corresponding author.

Email address: lubos.kascak@tuke.sk

into the coating.

Due to the diffusion of iron and alloying with zinc, the final coating contains around 90% zinc and 10% iron. Due to the alloying of zinc in the coating with diffused iron, there is no free zinc present in the galvanneal coating. HDGA coatings contain less aluminium than HDGI coatings, about 0.15 to 0.4 wt-%. Using of surface-treated steel sheets in automotive industry causes problems in optimization of welding parameters. Pollution of welding electrode tips changes the contact resistances, which lead to negative influence on welds' quality as well as welding tips' lifetime (Zhang, 2006; Kaščák, 2013).

Hot-dip galvanized steel sheets are still the preferred material in car body constructions in the automotive industry. Currently, there is sufficient confidence to define appropriate welding parameters to obtain required quality of welds in two joined materials. However, limited work has been published for three thickness combinations, especially focused on the optimization of the welding parameters.

2. Methodology of Experiments

Double-sided hot-dip galvanized steel sheets DX51D + Z - EN 10142/2000 of 1.0 mm thickness made by U.S. Stell Košice, Ltd. were used for the experiments. An average thickness of zinc coatings measured by contact thickness gauge Quanix was 16.8 μm . The steel is suitable for deep-drawing and it is used for production of car body parts. The measured chemical composition of the observed materials and their basic mechanical properties declared by the producers are shown in Table 1 and Table 2. The chemical composition was measured by spectrometer Belec Compact port.

The dimensions of samples: 40 x 92 mm, were determined according to DIN 50 124 standard - Tensile Shear Test on Resistance Spot Welded; Projection Welded and Fusion Spot Welded Joints. The length of lapping was 32 mm. Six samples were prepared for each particular combination of welding parameters. Five of them were used for measuring of carrying capacities by tensile test and one of the samples was used for metallographic analyses. The samples were prepared by cutting against the direction of rolling. The surfaces of the samples were degreased in concentrated

CH_3COCH_3 . Resistance spot welding was carried out in laboratory conditions on a pneumatic spot welding-machine BPK 20 made by VTS ELEKTRO Bratislava. CuCr welding electrodes were used according to STN EN 25 821 standard. The diameter of working area of the electrode was $d = 5 \text{ mm}$.

The heat needed to create the coherence is generated by applying an electric current through the stack-up of sheets between the electrodes. Therefore, the formation of a welded joint, including the nugget and the heat-affected zone (HAZ), strongly depends on the electrical and thermal properties of the sheet and coating materials. A weld's formation can be linked to the electrical and thermal processes of welding. Controlling the electrical and thermal parameters is a common practice in resistance welding. The general expression of heat generated in an electric circuit can be expressed as

$$Q(t) = \int_0^t I(t) \cdot R \cdot dt \quad (1)$$

where Q is generated heat, I is welding current, R is electrical resistance of the welding circuit and t is welding time the current allowed to flow in the circuit (Zhang, 2006; Aslanlar, 2004).

Welding parameters (F_z – pressing force, T – welding time, I – welding current) for three steel sheets of material DX51D + Z - EN 10142/2000 of 1 mm thickness are shown in Table 3.



Figure 1. Welded joints of car body (Volkswagen)

Table 1. Chemical composition of material used [in %wt]

C [%]	Si [%]	Mn [%]	Al [%]	P [%]	S [%]	Cr [%]	Fe [%]
0.064	0.007	0.178	0.120	0.040	0.040	0.023	bal.

Table 2. Basic mechanical properties of material used (R_m – ultimate tensile strength, R_e – yield strength, A_{80} – elongation)

R_m [MPa]	R_e [MPa]	A_{80} [%]
max. 450	140-280	23

Table 3. Welding parameters of DX51D + Z - EN 10142/2000 steel

Welding parameters		Samples							
		A1	A2	A3	A4	B1	B2	B3	B4
Fz	[kN]	3	3	3	3	3	3	3	3
T	[per]	10	10	10	10	12	12	12	12
I	[kA]	6	6.6	7	7.7	6	6.6	7	7.7

The tensile test was carried out on tensile machine TIRA test 2300 manufactured by VEB TIW Rauenstein with the load speed of 8 mm/min according to DIN 50 124 standard. The structures of welded joints were observed on metallographic scratch patterns on a light microscope Olympus TH4-200.

3. Analysis of Results

3.1. Analysis of carrying capacity of welded joints

Only one type of joint occurs in all chosen parameters of welding-fusion welded joint, which was observed in tensile test and in metallographic analysis. The lowest carrying capacity of joint was measured in samples A1 that correspond to the lowest values of welding parameters ($I = 6$ kA, $T = 10$ periods). The highest values of carrying capacity was measured in samples B4, which were welded with the highest values of welding parameters ($I = 7.7$ kA, $T = 12$ periods). Dependency of average values of carrying capacities of spot welds F_{max} on used values of welding current I is shown in Figure 2.

Increasing values of welding current caused an increase in carrying capacities of spot welds linearly in both types of samples. Increasing the welding time from 10 periods to 12 periods has a positive influence on the values of carrying capacities of welded joints. Dependency of carrying capacities of spot welds F_{max} on welding current I in both periods $T = 10$ per. (2) and $T = 12$ per. (3) of welding can be expressed as

$$F_{max} = 1325.7I + 230.85; R^2 = 0.9726 \quad (2)$$

$$F_{max} = 702I + 6203.9; R^2 = 0.9331 \quad (3)$$

Increase in values of carrying capacity of joints influenced by increasing the welding time is shown in Table 4.

3.2 Metallographic analysis

During welding of galvanized steel sheets, Zn is melted and diffused into welding electrode tips (made of CuCr elements) which lead to creation of brass layer. Brass has higher electrical resistance than copper therefore the higher heat is generated in brass layer. The welding electrode tips get hotter as the dimension of the weld nugget decreases.

The weld nugget of the smallest dimensions within the evaluated series was observed in samples A1, which is in accordance with the measured values of load bearing capacity of the joints. No significant marks of welding tips on

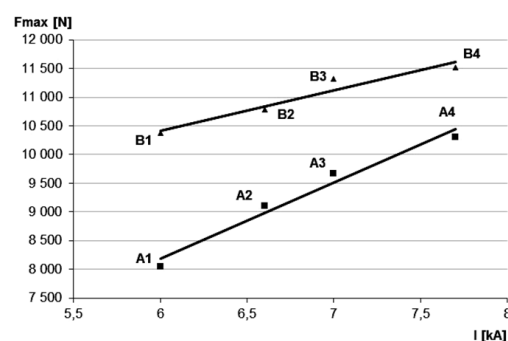


Figure 2. Dependency of average values of carrying capacities of welded joints F_{max} on welding current I

Table 4. Increase of carrying capacity of samples A in comparison with samples B (in %)

Samples A	Average values of carrying capacities [N]				
	(A1)	(A2)	(A3)	(A4)	
	8043	9103	9662	10306	
Samples B	(B1)	(B2)	(B3)	(B4)	
	10366	10788	11316	11510	
Difference in carrying capacity values in [%]		22.41	15.62	14.62	10.46

the surfaces of joined materials were observed. Macrostructure of A2 sample is shown in Figure 3. The quality of joint is sufficient; however, there occurred flashing of basic material (BM) on the upper side of the joint up to the depth of 50 μm , and on the lower side of the joint up to the depth of 150 μm . There can be observed remains of Zn layer on the transition from BM to the weld on the left side of the macrostructure. The same was observed in samples A3. Increasing of the welding current of 0.4 kA has no significant influence on the dimensions of weld nugget and occurrence of defects in welded joint.

Better quality of the weld of A4 sample in comparison with A2 sample is shown in Figure 4. No macroscopic or microscopic defects were observed in the weld.

Zn layer evaporated from the contact place of the electrode with BM. Flashing of BM was not observed and



Figure 3. Weld macrostructure of A2 sample, diameter of weld nugget $d = \varnothing 4.3 \text{ mm}$



Figure 4. Weld macrostructure of A4 sample, diameter of weld nugget $d = \varnothing 5 \text{ mm}$

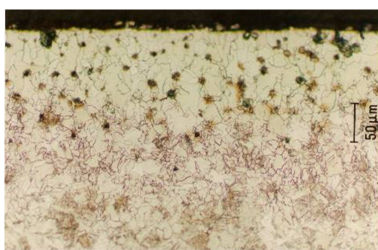


Figure 5. Macrostructure in the area of material surface, sample A4

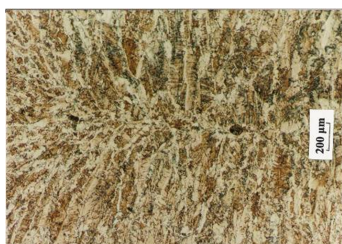


Figure 6. Microstructure in the centre of the weld, sample A4

microstructure of the place near the surface consists of ferrite and fuzzy pearlite as shown in Figure 5.

The middle of weld is well remelted with the symmetrically oriented dendritic structure – Figure 6.

Figure 7 shows structure of the weld with acicular polyedric ferrite.

Figure 8 shows transition of the weld and BM. Detail of the transition is shown in Figure 9. Fine-grained ferrite structure or fine-grained ferrite and fuzzy pearlite was formed between dendritic structure and BM.

The weld nuggets without any internal defects were observed in samples B1 as well as B2, as is shown in Figure 10. Unlike the samples A, significant electrode marks on the surfaces of joined materials occurred, which were caused by



Figure 7. Microstructure of the weld, sample A4

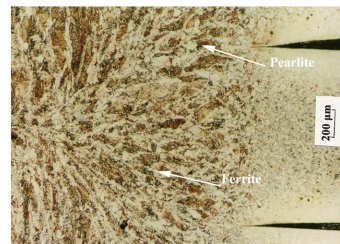


Figure 8. Transition from the weld to the base material, sample A4

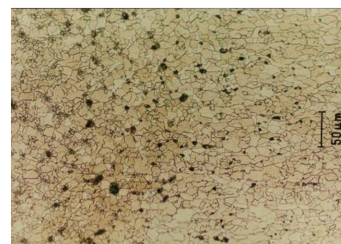


Figure 9. Microstructure of transition from the weld to the base material, sample A4

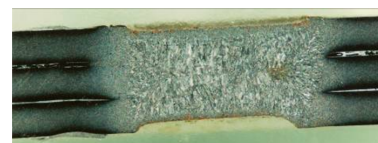


Figure 10. Microstructure of the weld, sample B2, diameter of weld nugget $d = \varnothing 5.5 \text{ mm}$

increasing the welding time. The minimal increasing of welding time of 2 periods led to increased load-bearing capacity of the joints, significant grain coarsening in the weld structure and significant deformation of material surface under welding electrode tips. The welded joint is without any defects in structure even on the surfaces of the sheets, only deformation under electrodes occurred, up to the depth of 200- 300 μm .

The attendant phenomenon of flashing is penetration of Zn into the weld is shown in the area on Figure 11. Accumulation of Zn near the melted surface is shown in the area on Figure 12. The presence of Zn was confirmed by EDX analysis by scanning microscope.

Occurrence of cavities and pores in the middle of the weld nugget was observed in the macrostructure of samples B3. These occurrences are commonly caused by gaseous bubbles (as well as evaporation of Zn layer) and from solidification shrinkage. These internal defects are also documented in the microstructure of weld metal in Figure 13. The direction of solidification in the weld metal can be readable. Change of HAZ size due to the heat input was observed.

Figure 14 shows the weld macrostructure of sample B4 with two cavities of elliptic form of size about 1 mm caused by solidification shrinkage. Flashing of BM into the depth 200-300 μm was observed.

Furthermore, a crack in the middle of the weld of about 0.25 mm occurred, which is shown in Figure 14. Increasing the welding current led to increased grain size in the weld nugget, height of weld nugget and an increasing of portion of acicular ferrite and pearlite in the structure of weld nugget. Load bearing capacity of the samples was increased too. Increasing of welding current is limited up to the value of $I = 7\text{kA}$, because further increasing of welding current ($I = 7.7\text{kA}$) caused internal defects such as cavities in the middle of weld nugget and external defects such as significant marks of welding electrode tips on the surfaces of the joined materials. The above-mentioned defects had no negative influence on the load bearing capacity of welded joints (Figure 2), but their occurrence is not acceptable according to valid standards.

4. Conclusions

Resistance spot welding is one of the most used welding processes for joining car body parts in automotive industry, because it is a simple and cost-effective joining method. Spot welding provides accelerated speed and adaptability for automation in high-volume and high-rate production. Understanding process parameters, such as weld size, weld indentation, sheet separation and weld residual stresses, will improve the weld quality during fabrications.

The paper dealt with resistance spot welding of three car body galvanized steel sheets with various welding parameters.

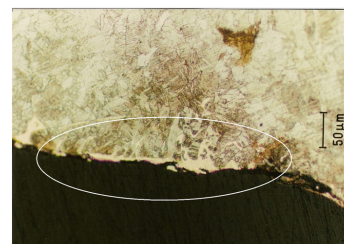


Figure 11. Penetration of Zn into the melted surface, sample B2



Figure 12. Accumulation of Zn on the weld surface, sample B2

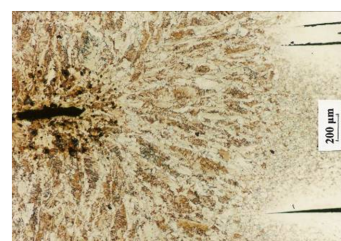


Figure 13. Crack in the centre of the weld, sample B4



Figure 14. Macrostructure of the weld, sample B4

On the basis of the experiment results it can be stated that only fusion weld joints occur within all chosen parameters of resistance spot welding. Increasing the parameters of the welding current caused an increase in values of carrying capacities linearly with the high values of correlation.

Within the carrying capacities evaluation, the optimal welding parameters are: $F_z = 3\text{kN}$, $T = 12$ periods and $I = 6.6\text{kA}$ (samples B2).

These welding parameters are also suitable according to results of metallographic analysis of welded joints on three 1 mm thick sheets of DX51D+Z - EN 10142/2000. When using the above mentioned parameters, welded joints are of high quality, they have high quality surface, optimal structure and no internal defects.

References

- Aslanlar, S. 2006. The effect of nucleus size on mechanical properties in electrical resistance spot welding of sheets used in automotive industry. *Materials and Design*. 27, 125-131.
- Harlin, N. , Jones, T.B., and Parker, J.D. 2003. Weld growth mechanism of resistance spot welds in zinc coated steel. *Journal of Materials Processing Technology*. 143-144, 448-453.
- Hilditch, T.B., Speer, J.G., and Matlock, D.K. 2007. Effect of susceptibility to interfacial fracture on fatigue properties of spot-welded high strength sheet steel. *Materials and Design*. 28, 2566-2576.
- Kaščák, L., Mucha, J., Slota, J., and Spišák, E.. 2013. Application of modern joining methods in car production. *Oficyna Wydawnicza Politechniki Rzeszowskiej, Rzeszów, Poland*.
- Kaščák, L. and Spišák, E. 2007. Joints of thin sheets made by forming and resistance spot welding: evaluations of properties. *Proceeding of IDDRG 2007, Forming the future : Innovations in sheet metal forming, Gyor, Hungary, May 21-23, 2007, 545-550*.
- Matta, M., Gatial, M., Tumuluru, D.M., Kaščák, L., and Viňáš, J. 2009. Optimization of resistance spot welding parameters for hot-dipped galvanized DP600 steel. *Stará Lesná, Bratislava, Slovakia, p. 1-14*.
- Zhang, H. and Senkara, J. 2006. *Resistance Welding: Fundamentals and Applications*, Taylor and Francis Group, New York, U.S.A.